



Assessing urban-heating impact on street tree growth in Berlin with open inventory and environmental data

Alexander Gideon Hurley¹ · Ingo Heinrich^{1,2,3}

Accepted: 4 October 2023 / Published online: 25 October 2023
© The Author(s) 2023

Abstract

Excess heat (i.e., Urban Heat Island; UHI) and other urban conditions affect tree physiology with outcomes from enhanced growth to mortality. Resilient urban forests in the face of climate change require species-specific understanding of growth responses. However, previous studies assessing growth dynamics were primarily based on remote sensing of communities rather than individuals, or relied on labor-intensive methods that can limit the spatial coverage necessary to account for highly variable urban growing conditions. Here, we analyze growth dynamics of common urban street tree species over time and across space for Berlin (Germany) combining dendroecological (temporal) and inventory assessments (spatial). First, we show annual increments increased across the 20th century for early (i.e., young) growth. Second, we use an approach relying on open inventory data to identify growth potential in relation to excess heat while accounting for age, potential management effects, and the urban fabric (i.e., planting area; building density, height; available soil nutrients) with generalized additive models for the ten most abundant species. Our analyses showed that younger trees may benefit from increased temperatures, while older individuals feature lower growth at greater UHI magnitudes. Furthermore, planting area as well as building density modulate growth responses to temperature. Lastly, we discuss management implications in the context of climate change mitigation, considering that younger trees are predominantly located at UHI “hot spots” and will undergo the observed age-dependent shift in temperature-growth sensitivity. By relying on increasingly available open data, our approach here is or will be transferable to other urban regions.

Keywords Tree species selection · Urban forest · Space-for-time analysis · FAIR data

Introduction

Excess heat common for cities (i.e., Urban Heat Island, UHI, Oke 1982), combined with other urban conditions, affects tree physiological functioning with outcomes ranging from enhanced growth to early senescence, branch die-back, and even mortality (Au 2018; Gillner et al. 2014; e.g., Hilbert et al. 2019). Thus, assessing the effect of increased temperatures on trees, as part of urban green infrastructure, is instrumental for understanding as well as adapting to current

and expected conditions in this century (Ward and Johnson 2007), especially considering ever more urbanized societies and the potential for UHI effects to compound with more frequent atmospheric drought (Brune 2016; Norton et al. 2015; Roloff et al. 2009).

The UHI effect, i.e., the difference between urban and adjacent rural (air) temperatures, has been intensively studied for several decades (cf. Oke 1982; Stewart 2011). It is typically related to the structure and density of urban land-use (Kuttler et al. 2015), which can be characterized through local climate zones, and modulated by physiographic and urban characteristics, such as vicinity to water bodies, predominant wind and street direction, etc. (Stewart and Oke 2012); yet, the physical basis for the excess heat in cities is to a large extent found in the altered surface energy balance as the proportional cover of vegetation decreases compared to rural (or reference) systems (Hertel and Schlink 2019; Oke 1992). In temperate climates, this results in strongest UHI magnitudes at night (cf. Fenner et al. 2014). For example,

✉ Alexander Gideon Hurley
agl.hurley@gmail.com

¹ Geoforschungszentrum Potsdam, Climate Dynamics and Landscape Evolution, Potsdam, Germany

² Deutsches Archäologisches Institut, Dendroclimatology, Berlin, Germany

³ Geography Department, Humboldt-Universität zu Berlin, Berlin, Germany

Berlin features the most intense UHI in Germany due to its large extent and development intensity with an average air temperature increase of around 5 K at night-times (2001–2010) with maxima of up to 11 K (Fenner et al. 2014) in urban vs. rural areas.

Increased air temperatures due to UHIs can affect tree growth through altering several physiological processes across plant organs directly or indirectly (Dusenge et al. 2019). Generally, reaction times at cellular level increase with temperature up to a maximum, after which a drop in enzymatic activity results in a species-dependent optimum curve (Arcus et al. 2016; Parent et al. 2010). In leaves this optimum response is reflected in the net assimilation rate of carbohydrates, as a balance of photosynthesis and respiration, with losses exceeding gains more rapidly with increasing temperatures (Long 1991). These responses vary between species (Tjoelker et al. 2001) as well as intra-specifically due to local acclimation, i.e., a shift of optimum temperature responses after prolonged exposure (Yamori et al. 2014), and threshold temperatures before tissue damage occurs (for review see Geange et al. 2021). High temperatures in temperate areas are often coincident with low relative air humidity (i.e., large vapor pressure deficit), which in turn can decrease stomatal conductance governing the majority of gas exchange in leaves (Grossiord et al. 2020), and thus the capacity for photosynthesis. Under prolonged stomatal closure (or decreased conductance) with high temperatures, trees may thus face decreased growth (in subsequent years) or even starvation as their carbohydrate reserves are depleted yet not replenished at sufficient rates (McDowell et al. 2008). Furthermore, air (and soil temperatures) affect the initiation, speed and cessation of cambial activity, and thus radial growth throughout a growing season (e.g., see Begum et al. 2013; Rathgeber et al. 2016). Radial growth is increasingly considered to be limited by wood formation dynamics and their relation with environmental drivers, rather than solely by photosynthetic activity (Körner 2015). In particular, the availability of soil water is critical for cell expansion (e.g., Peters et al. 2021) and most likely limits radial growth before photosynthesis (Fatichi et al. 2014); however, this water availability is again linked to local climate as higher temperatures drive evaporation and thus may contribute to the depletion of soil water storage, impeding growth.

Several urban tree species have been shown to have tendencies of enhanced growth rates and/or productivity compared to rural conspecifics (e.g., Briber et al. 2015; O'Brien et al. 2012), which is typically attributed to increased temperatures (Jia et al. 2018; Pretzsch et al. 2017), however, a broad range of effect sizes and signs (i.e., reduced growth) specific to species and location are also commonly reported alongside (e.g., Berland 2020). For instance, Zhao et al. (2016) showed that

productivity rates, as a proxy for growth, increased within urban clusters as urbanization intensifies using remotely sensed vegetation indices. Furthermore, Moser-Reischl et al. (2019) identified positive associations between air temperature and radial growth for two species commonly selected by urban planners (*Tilia cordata* Mill., *Rubinia pseudoacacia*) in Munich. Similarly, for Berlin, Dahlhausen et al. (2018), identified enhanced growth in highly urbanized environments for *T. cordata*, the most abundant tree of the city, which they attributed to the UHI effect, while intermediate development intensity was adverse for tree growth. By contrast, Gillner et al. (2014) highlight decreased growth for *Acer* species (*A. platanoides* and *pseudoplatanus*), *Platanus x hispanica* and *Quercus rubra* with higher summer temperatures of the preceding year, especially when compounded with drought, in another major German city (Dresden). These differences in growth trends may result from contrasting species-specific responses to increased temperatures, but are indeed affected by other (time-varying) factors and stochastic processes, such as water availability, pollution and road-salt loading, structural impedance by infrastructure, or management, etc. (Pauleit et al. 2002; Quigley 2004; Randrup et al. 2001; Rhoades and Stipes 1999).

Multiple of the aforementioned studies applied space-for-time substitutions or time series comparisons to quantify temperature and excess heat on growth for a given region. However, they typically compared trees grouped using qualitative or summary descriptors of sampling sites, disregarding the spatial and/or temporal variability in location-specific factors noted above that may affect growth of individual trees. This can hinder the extrapolation from individual sampling sites toward predicting effects across entire urban areas and tree stocks, especially when studies rely on labor-intensive methods, reducing sample sizes and coverage of species and space. A lack of co-located environmental variables (i.e., measured *in situ* or modelled) at pertinent spatial scales can further exacerbate these limitations, as noted, for instance, by Wohlfahrt et al. (2019) for air temperature and urban tree leaf phenology, which may lead to incorrect inferences and interpretations for the role of climate change on growth/productivity. Indeed, even neighboring trees' exposure to excess heat may differ substantially as the urban fabric that controls their microclimate varies at short distances and across time (e.g., shading at low and high sun angles through days and seasons, extent and characteristics of sealed surfaces, etc.). It is thus likely that the varying and even contrasting growth responses observed for urban trees across and within studies are at least modulated by some confounding factors and exacerbated by lack of co-located environmental variables, making the attribution to a single driver, such as excess heat, more difficult and possibly less accurate.

These limitations could be overcome by developing extensive dendroecological surveys (i.e., incremental growth) and/or inventories (single or repeat) combined with environmental data with adequate spatio-temporal coverage and resolution. Environmental data such as surface and air temperatures from remote sensing products and process-based models have been used as a basis for assessing phenological and growth differences between and within tree species. For example, Dale and Frank (2014) and Locosselli et al. (2019) extracted remotely-sensed landsurface temperatures in the vicinity of manually sampled trees as a proxy for microclimatic conditions that influence growth. Similarly, Vo and Hu (2021) use remote sensing imagery with a downscaling modelling scheme to develop canopy-level temperature data for further analyses. Tree inventories are logistically and financially more feasible compared to extensive dendroecological surveys, and - together with environmental data - are increasingly more available (e.g. Ossola et al. 2020) due to open data policies and their value being recognized across domains for urban greenspace planning and adaptation (Hansen et al. 2019; Monteiro et al. 2020). Berlin, as one of the greenest cities in Europe, provides an openly accessible tree inventory, with spatio-temporal environmental data sets relevant to tree growth. It features nearly 700000 individuals covering 94 genera and some 600 species and/or cultivars, listing information on location, stem diameter (at breast height; *DBH*), and stem height, among other variables, for the majority of street and park trees. For this study, our objective was to assess the impact of excess urban heat, i.e. the UHI effect, on street tree growth (*DBH*) using this openly available inventory data set, complemented by additional open data sources with high resolution and good spatial coverage, as well as incremental growth data from tree cores. The assessment relied on flexible statistical models that could capture species and location-specific responses to heat and other urban factors. Specifically, we aimed to (1) assess heat exposure of the most abundant species; (2) determine the impact of (excess) heat on stem growth across tree age classes with a space-for-time substitution; (3) highlight the role of location-specific environmental factors in mediating temperature responses.

Methods

Study area

Berlin is one of the largest metropolitan areas in Central Europe (892km²) with a population of approximately 3.6 million, and a maximum extent of 38km in North-South and 45km in East-West directions. It is located in North-Eastern Germany, and lies in the temperate zone with warm-humid climate (Dfb) according to the updated

Köppen-Geiger classification (Beck et al. 2018), with mean annual temperature of approximately 10 °C and precipitation of 575mm (Tempelhof weather station, DWD). Berlin features low relief (approximately 30m to 60m with 120m at solitary peaks), and is centered around a glacial outwash valley (sands, gravel), bordered by two plateaus consisting of glacial till and clay in the North-East and South, as well as sands in the South-West. The city provides extensive public green space covering around 30% of its area (SUVK and Berlin 2019), with an extensive urban forest of nearly 700000 publicly-managed trees along streets, in parks and in riparian areas (Fig. 1).

Data sources

An overview of data used for models, including sources, types, and application, is provided in Table 1, with detailed descriptions in the following subsections.

Street trees

Berlin's open data provided tree inventories including species, age, location, and circumference which was transformed into diameter. Note that only street trees in urban, not rural areas or within green spaces, were considered here, but individual trees may grow along streets adjacent to green spaces and parks of varying sizes. Implausible observations, possibly from erroneous data entry, were removed. Additional manual data processing for quality control was done with a bespoke software *datacleanr* by Hurley et al. (2022), where obvious outliers or clearly interpolated data were removed. The latter was deemed necessary, as several observations in multiple city districts were derived by linear relationships (i.e., straight-line),

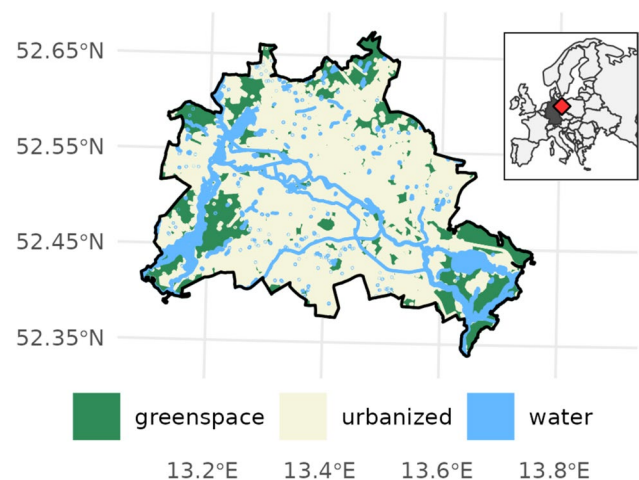


Fig. 1 Berlin's generalized land-use derived from SUVK and Berlin (2019) and location within the European context (inset)

Table 1 Data description used for maps, visualizations and analyses. Resolution and radius are in *m*, the latter is the buffer in which data was averaged around each tree. A zero-radius refers to a point extrac-

tion from categorical and location specific data. Polygons with radius data were rasterized to a resolution of 5 *m*

Name	Accessed	Type	Unit	Res (m)	Radius (m)	Source	Reference
Street Trees	Oct '20	Point				https://daten.berlin.de/	
UHI Berlin	Dec '19	Raster	°C	500	150	https://yceo.yale.edu/research/global-surface-uhi-explorer	Chakraborty and Lee (2019)
Berlin Climate Model, Air temperature 2015 (Umweltatlas)	Feb '21	Polygon	°C	5	150	https://daten.berlin.de/	
UrbClim ERA5 Model Output (ECMWF, UCSC)	Mar '21	Raster	°C	100	150	https://cds.climate.copernicus.eu/	De Ridder et al. (2015)
Berlin Land-use	Apr '21	Polygon				https://daten.berlin.de/	
Copernicus CORINE CLC	Mar '21	Raster		100		https://land.copernicus.eu/	
WUDAPT LCZ	Oct '20	Raster		100	150/300	https://www.wudapt.org/continental-lcz-maps/	Demuzere et al. (2019)
Berlin Vegetation and Building Height	Oct '20	Polygon	<i>m</i>	5	150/300	https://daten.berlin.de/	
Berlin Soil Nutrients, Bodenkundliche Kennwerte 2015 (Umweltatlas)	Nov '20	Polygon	<i>mol m⁻²</i>		0	https://daten.berlin.de/	
Planting Bed Area	Oct '20	Polygon	<i>m²</i>		0	https://daten.berlin.de/	
Berlin Soils	Oct '20	Polygon			0	https://daten.berlin.de/	
Berlin Districts	Oct '20	Polygon				https://daten.berlin.de/	
Berlin Transport Network	Feb '21	Polygon				OpenStreetMap Overpass API	
Berlin Water (Ways)	Feb '21	Polygon				OpenStreetMap Overpass API	

which do not capture the ontogenetic growth dynamics of trees, and leave no variation related to variables other than age. All of these operations were recorded, and can be viewed and reproduced via the code linked in the Online Resource 1. Lastly, observations with unlikely diameter-age combinations were identified via the residuals of a generalized linear model between diameter and age with a Gamma log-link distribution: if individual residuals exceeded seven times the median absolute deviation of all residuals, they were removed. The median absolute deviation (MAD) is comparable to the inter-quartile range, yet more robust to outliers:

$$MAD = \text{median}(\| X_i - \text{median}(X) \|) \quad (1)$$

Similar cut-off approaches are frequently applied in allometric and trait databases. We considered this approach (i.e., $MAD \cdot 7$) conservative, and necessary given the presence of clearly erroneous data. The approach and impact thereof are visualized in the Online Resource 1 (Section Data quality control). Table 2 shows the binned distribution of genera across age classes. Final samples applied in models were smaller, following the availability of ancillary data for a given observation, and limited to

a maximum age of 125 years to increase confidence in reported values, and ultimately model estimates.

Temperature/UHI data

Temperature and UHI data were summarized temporally either by the provider or manually to provide a characteristic representation of (excess) heat during summer at different times (morning, afternoon/day, night), from which tree averages (radius of 150 m) were calculated (Fig. 2). Two urban air temperature (Berlin Environmental Atlas, UrbClim) and one surface UHI data set (MODIS) were tested as explanatory variables in generalized additive models (see Section GAMS). The air temperatures from the Berlin Environmental Atlas (EnvAt) are processed model outputs (FITNAH-3D; cf. Gross 1994) that are representations of typical summer conditions at 0400, 1400 and 2200 h at 2 m height; these data are provided at city block basis (spatial polygons), from which weighted averages were extracted after rasterizing (5 m resolution). The model was assessed by comparing microclimatic patterns from model outputs against two measurement campaigns for a representative location (greenspace – building transition), which show

Table 2 Binned age-distribution for street tree genera in Berlin data set, and entries missing age information

Genera	(0,30]	(30,60]	(60,90]	(90,120]	(120,150]	150+	Total (n)	Missing (n)
<i>Tilia</i>	40128	60854	34599	4390	120	11	140232	130
<i>Acer</i>	23306	33771	10220	1798	62	17	69330	156
<i>Quercus</i>	8686	16107	5721	2595	562	157	33873	45
<i>Platanus</i>	4467	11836	4784	1449	805	68	23425	16
<i>Aesculus</i>	4464	7064	5566	1211	91	25	18427	6
<i>Betula</i>	2469	7155	897	36	2	1	10572	12
<i>Fraxinus</i>	4324	3332	742	131	6	0	8543	8
<i>Robinia</i>	2494	4523	857	83	3	1	7975	14
<i>Carpinus</i>	3905	2349	176	4	0	0	6466	32
<i>Prunus</i>	3792	2121	111	12	0	0	6067	31
<i>Populus</i>	639	3559	991	279	17	14	5515	16
<i>Pinus</i>	422	1349	463	27	0	1	2269	7
Other	22337	12620	1799	448	61	17	37554	272
Marg. Totals	121433	166640	66926	12463	1729	312	370248	745

good agreement (see <https://www.berlin.de/umweltatlas/klima/klimaanalyse/2014/methode/>; only available in German). We decided to use the raw air temperatures from this data set, rather than calculating excess heat, i.e., an UHI measure, as the model outputs are limited to Berlin's extent and thus do not cover extensive rural areas (see Eq. 2). UrbClim air temperatures are hourly model outputs (100 m resolution, 2 m height, De Ridder et al. 2015) based on ERA5 re-analyses data (ECMWF) for which observations from the hottest month available (June, 2011) were averaged to hours equivalent to Berlin Environmental Atlas (referred to as Berlin EnvAt) data by using a window of \pm 1 hour (i.e., 0300 to 0500, etc.). The model domain extends beyond Berlin's city limits into adjacent rural areas. A land-use and land-cover mask (CORINE; European Union, Copernicus Land Monitoring Service 2018, European Environment Agency) was applied to define urban and rural/forested areas within and outside the city. Using this mask was deemed reasonable as Berlin's built-up area has not changed markedly over the past 50 years, i.e., about 52 to 61% (Mohamed 2017). The excess heat was then calculated as

$$UHI_{x,y} = T_{Air_{2m}, x,y} - \overline{T_{Air_{2m}, Rural}}, \quad (2)$$

where T is temperature ($^{\circ}C$) x and y define an urban grid cell. The model outputs have been extensively applied and validated for several cities (De Ridder et al. 2015; Lauwaet et al. 2016; Sarkar and De Ridder 2011; Zhou et al. 2016). The MODIS-derived surface UHI data set by Chakraborty and Lee (2019) (referred to as MODIS) estimates its measure in a similar fashion and the reader is referred to the detailed description therein. In brief, the underlying algorithm calculates the difference between urban and rural land surface temperatures for so-called urban clusters. The extent of urban areas is based on MODIS land-use data from 2002

(also considered unproblematic, see above). A filtering step in the algorithm ensures that UHI data are only generated for urban clusters where biased estimates are least likely (e.g., clusters excluded where no rural pixels were present, or where elevation differences between urban and rural pixels is greater than 50 m). Note this data set provides day and night-time averaged UHI estimates at 500m resolution, which were extracted for the hottest summer in this record (2007).

Ancillary environmental data

Following the general approach described above, four ancillary covariates next to a temperature measure were employed in models; these were chosen due to their availability at high spatial resolution and coverage, and/or because their influence on growth was previously identified in literature or their likely impact could be deduced using ecophysiological principles. We included planting bed area and the sum of exchangeable basic cation as a proxy for soil nutrient availability (point extractions), adjacent building height (rasterized to 5 m resolution), as well as the proportional coverage of local climate zone 6 (LCZ6; open arrangement of low-rise buildings of 1 to 3 stories, pervious land cover, low plants and scattered trees, see Demuzere et al. (2019) and Stewart and Oke (2012) for details). Local climate zones integrate multiple characteristics of the urban fabric into individual categories and are widely available in products such as the WUDAPT dataset (Demuzere et al. 2019), easily accessible for researchers and practitioners. We selected this class for two reasons: (1) abundance – LCZ6 shows the greatest spatial coverage when considering the averaging radius we applied around trees and thus we were able to retain more observations for subsequent analyses; (2) previous research indicated that street tree growth for *T. cordata*

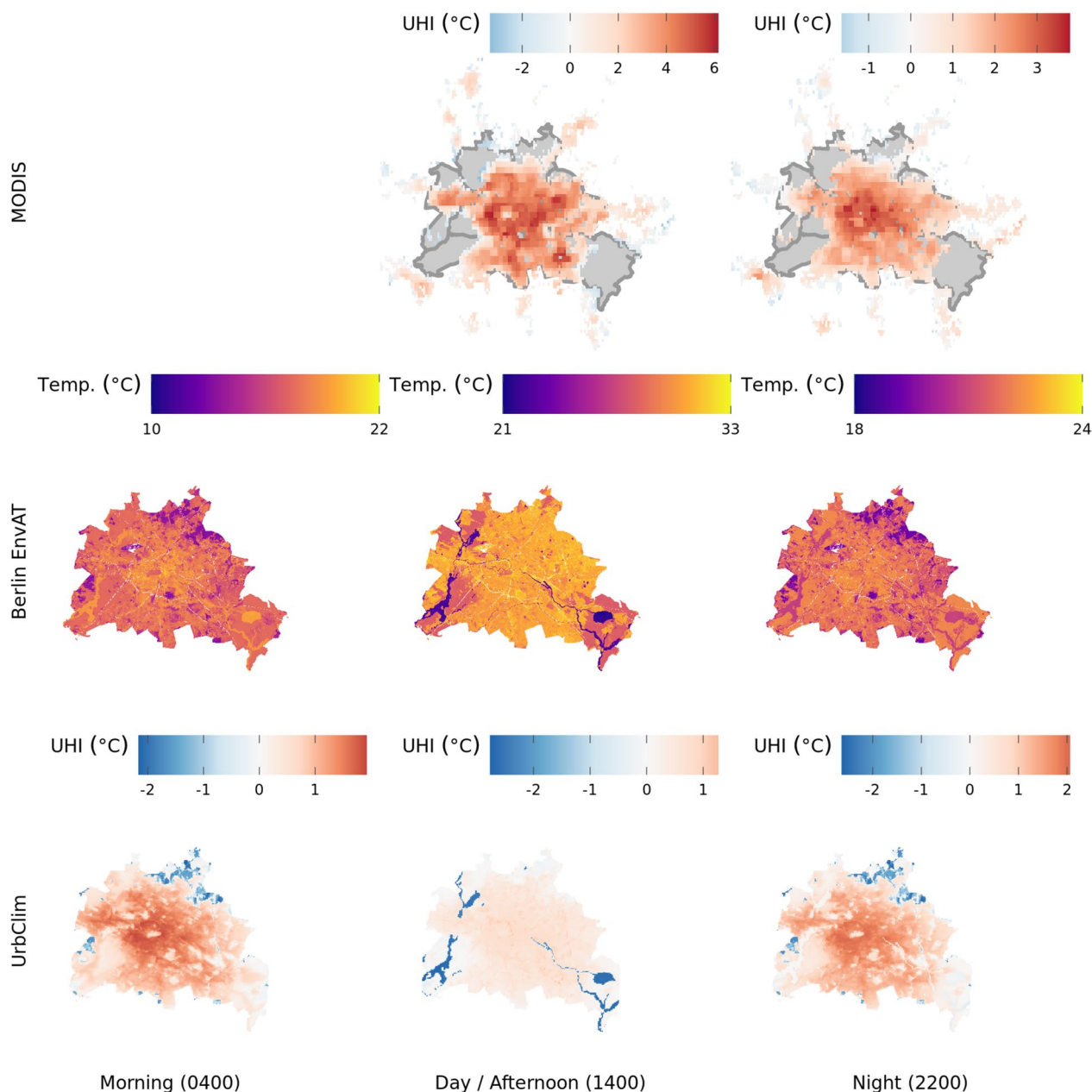


Fig. 2 Overview of data sets used for assessing the relationship between temperature and tree growth, with data sources in rows and averaged time intervals in columns. Note the varying spatial coverage and resolution as noted in Table 1

within medium housing density in Berlin varied most, which was related to strongest sensitivity for growing conditions or exposure to most extreme conditions (Dahlhausen et al. 2018), and thus some degree of relationship was to be expected with the LCZ6 class.

General approach: space-for-time analyses

We modeled the stem diameter (*DBH*) of Berlin's ten most abundant species (contingent to ancillary data availability)

in relationship to their location, age, a measure of (excess) heat (UrbClim by De Ridder et al. 2015; Berlin Environmental Atlas models; MODIS-derived surface Urban Heat Island by Chakraborty and Lee 2019), and additional environmental covariates with generalized additive models (GAMs, see Section GAMs for details). Covariates were extracted at 150 and 300m to infer the impact of reference scale of the urban fabric on tree growth. From all tested models the most suitable (i.e., parsimonious with highest explanatory power) was employed for further analyses.

Dendrochronological sampling

To contextualize tree growth patterns between age groups derived from Berlin's inventory data, we drew upon a recently established data set from Schneider et al. (2021), who sampled several common tree species across a rural-urban gradient. For our purposes, we grouped trees sampled in parks, green spaces and along streets into a single urban category, and focused analyses on these (Table 3). Note that Schneider et al. (2021) refer to these sampling locations as sub-urban and urban. Their analyses showed strong relationships between ring-width indices, climate parameters and a measure of urbanity derived from the proportion of sealed surfaces and building fraction. Thus it can be derived that the Berlin city tree-growth data applied here had a sufficient "urban imprint" relevant for our analyses. In brief, the data was derived as follows. Two to three cores were extracted at breast height from each tree. These were then prepared using standard dendroecological methods (i.e., mounting, sanding, measuring), and cross-dated with TSAP-Win™ and COFECHA (Holmes et al. 1986), producing mean tree series of incremental growth. Additionally, cambial age of each increment was established by counting years from the inner most ring at the pith ($a = 0$) outward; on tangentially bored cores, missing rings to the pith were estimated.

Statistical analyses

GAMs

We applied hierarchical generalized additive models (GAM) to estimate the relationship of several covariates with stem diameter growth (DBH). GAMs, as an extension of generalized

Table 3 Overview of urban sampling locations and species sample sizes (n). Individual trees were sampled two or three times to obtain a mean-tree ring width series

Location	Species	n
Alpenrose	<i>Quercus robur</i>	15
Grünanlage Britz-Süd	<i>Fagus sylvatica</i>	17
Grünanlage Britz-Süd	<i>Pseudotsuga menziesii</i>	17
Grünanlage Britz-Süd	<i>Fraxinus excelsior</i>	14
Grünanlage Britz-Süd	<i>Pinus sylvestris</i>	16
Grünanlage Britz-Süd	<i>Larix decidua</i>	16
Grünanlage Britz-Süd	<i>Tilia Cordata</i>	16
Grünanlage Britz-Süd	<i>Quercus robur</i>	15
Grünanlage Britz-Süd	<i>Quercus petraea</i>	21
Hasenheide	<i>Quercus robur</i>	12
Hasenheide	<i>Quercus robur</i>	14
Spielplatz Weigandufer & Wildenbruchplatz	<i>Fraxinus excelsior</i>	19
Werrastraße	<i>Fraxinus excelsior</i>	12

linear models (Wood 2017), allow modeling response variables as parametric and non-parametric combinations of smoothed explanatory covariates, and can assume non-normal response distributions. These smooths are constructed by summation of base functions of varying complexity and form, analogous to scatterplot smoothing (Hastie and Tibshirani 2017), which provides a high degree of flexibility, ideal for fitting ecosystem dynamics which are rarely linear (Pedersen et al. 2019), or correctly represented with deterministic functional forms (e.g. quadratic equations). In general, a GAM can be written as:

$$E(Y) = g^{-1} \left(\beta_0 + \sum_{i=1}^n f_i(x_i) \right), \quad (3)$$

and

$$y = E(Y) + \varepsilon, \quad (4)$$

where Y is taken from an appropriate distribution and corresponding link function g , β_0 is the intercept and f_i represents a smooth function of a predictor (Pedersen et al. 2019), and $\varepsilon \sim \mathcal{N}(0, \sigma^2)$. Nested data structures (e.g., city districts) can be accounted for by introducing random effects, while spatial dependence between observations can be accounted for by constructing smoothing functions with, for instance, northings and eastings (cf. Wood 2017). All models were implemented in R (Core Team R 2021) using functions available in the package `mgcv` (Wood 2017).

Dendrochronological analyses

We assessed trends in annual growth dynamics of urban trees across the 20th century for 1920–1960 and 1961–2001 (similar temporal grouping as Dahlhausen et al. 2018 and Pretzsch et al. 2017). Given the small sample sizes across species and potential for site-specific differences, we grouped all individuals and focused on inferring age-dependent growth patterns for these trees in general. We used a hierarchical GAM implemented in `mgcv::gam()` to leverage auto-correlation structures made available through the package `nlme` (Pinheiro et al. 2021) to account for individual variation across sites and species. Annual growth was modeled as:

$$g(\Delta r_i) = f(\text{year}_i) + f_j(\text{cambial age}_i) + c_{i,j} + \tau_{i,k} + e_i \quad (5)$$

where $g()$ is a log-link for $\Delta r \sim \text{Gamma}$, Δr is the annual radial increment for observation i . A global temporal (by year) and time-dependent ($j, \leq 1960$ or > 1960) trend in cambial age were implemented with thin plate regression splines (default smoothing function in `mgcv`); c_j is a time-group dependent intercept, while τ represents a matrix of random effect coefficients for k species to account for differences in growth patterns, and $e_i = \varphi e_{i-1} + \varepsilon_i$. A 3rd-order autocorrelation-moving average (ARMA) correlation

structure was applied (i.e., $\varphi(3, 1)$) to account for the dependency of Δr across years for each tree, as is frequently the case for tree growth (e.g., see Fritts and Swetnam 1989). Similar model structures, although not based on GAMs, have been applied by, for example, Pretzsch et al. (2017). The detailed implementation for this model is given in the code linked to in the Online Resource 1. Δr was then derived for a range of cambial ages, and averaged for both time groups, allowing a comparison of recent to earlier growth. We acknowledge that tree cores obtained at breast height do not represent absolute tree age. However, here they serve as a proxy for growth between young ($\gtrsim 1960$) and older individuals to contextualize growth patterns inferred from the larger-scale tree inventory.

Stem diameter model development and selection

We focused the analyses on the ten most abundant species after data quality control with a minimum of 10000 observations to ensure greatest possible spatial coverage and to increase confidence in estimates, totaling 218329 trees, with Table 4 showing species-specific sample sizes.

The diameter (*DBH*) of these species was modeled using GAMs as follows:

$$g(DBH_i) = f(x_i, y_i) + f_j(age_i) + f_j(temp_{t,i}, age_i) + f(covariate_i) + c_{i,j} + \tau_{i,k} + \varepsilon_i \quad (6)$$

$$g(DBH_i) = f(x_i, y_i) + f_j(age_i) + f_j(temp_{t,i}, age_i) + c_{i,j} + \tau_{i,k} + \varepsilon_i \quad (7)$$

$$g(DBH_i) = f(x_i, y_i) + f_j(age_i) + f(covariate_i) + c_{i,j} + \tau_{i,k} + \varepsilon_i \quad (8)$$

$$g(DBH_i) = f(x_i, y_i) + f_j(age_i) + c_{i,j} + \tau_{i,k} + \varepsilon_i \quad (9)$$

Table 4 Ten most abundant species and total sample size (n) for which GAM models were developed. Note that ancillary data availability across variables determined final sample sizes in individual models

Species	n
<i>Tilia cordata</i>	58803
<i>Acer platanoides</i>	41090
<i>Platanus acerifolia</i>	22358
<i>Quercus robur</i>	20152
<i>Tilia platyphyllos</i>	16992
<i>Aesculus hippocastanum</i>	13899
<i>Tilia intermedia</i>	12926
<i>Tilia intermedia 'Pallida'</i>	11016
<i>Tilia euchlora</i>	10785
<i>Acer pseudoplatanus</i>	10308

where $g()$ is a log-link for $DBH \sim \text{Gamma}$, and i, j are indices for observations and species, respectively, and t refers to an (excess) heat measure from UrbClim, Berlin EnvAt or MODIS at different times (morning, afternoon/day, night; see Section [Temperature/UHI data](#)); c is a species-dependent intercept, while τ represents a matrix of random effect coefficients for k districts to account for differing management regimes across the city. A global spatial smooth $f(x_i, y_i)$ (representing projected coordinates in UTM) via a Gaussian process (cf. p. 242 in Wood 2017) was included to account for the spatial structure of observations, which reduced auto-correlation of model residuals considerably (see Online Resource 1). These were compared to a sub-set of models without a spatial component (cf. Eq. (7), and Fig. 4 but not further discussed there). We also tested a suite of models without the spatial smooth for comparison.

Furthermore, we implemented the interaction between temperature and age (i.e., $f_j(temp, age)$) as tensor smooths (Wood 2006) to account for the different variable scales (i.e., units); all models were also tested without this interaction using a thin plate regression spline smooth for temperature (not shown in equations above). The functions f_j are for species-specific smooths (i.e., with individual smoothness penalties and functional shapes as detailed by Pedersen et al. 2019). The covariates for planting bed area and soil nutrient availability were log-transformed to account for their skewed distribution, improving the estimation of coefficients for their respective basis functions. Note, that Eq. (9) was considered as the appropriate null model for interpretations, and a model including all covariates and the temperature-age interaction was tested as a saturated model. Models were implemented with `mgcv::bam()` (Li and Wood 2020; Wood et al. 2017) and readers are referred to the detailed implementation in the code linked to in the Online Resource 1. Considering all combinations of (excess) heat measures and covariates (with point, as well as 150/300m extractions), a total of 158 models were applied. With these models, we derived age and species dependent *DBH* averages across a temperature measure from predicted values in 5-year age groups starting at 30, 45, 60, 75, 90

Model selection was based on explained deviance (similar to explained variance) and the Aikake's information criteria (AIC). The best model, considered having the highest explanatory power (highest explained deviance) and simplest structure (lowest AIC), was chosen for final analyses. Explained deviance assesses model fit in generalized linear modelling similar to explained variance in ordinary least squares modelling, but relies on a generalized form of residuals, i.e., deviance residuals (see Wood 2017). Deviance for the Gamma distribution is calculated as

$$D(y, \hat{\mu}) = 2 \cdot \left\{ \frac{y - \hat{\mu}}{\hat{\mu}} - \log\left(\frac{y}{\hat{\mu}}\right) \right\} \quad (10)$$

where y is the observed and $\hat{\mu}$ the expected value.

As the spatial extent and coverage varied between temperature and ancillary data, more complex models (and specifically those including planting bed area and MODIS temperatures) typically also had fewer total observations. While this prevented a full comparison with information-based model selection criteria like AIC, the appropriateness of models that differed only in their implementation of the temperature-age interaction (i.e., $f_j(temp_i)$ vs. $f_j(temp_i, age_i)$) could be assessed. For this reason, the suite of developed models presented above were limited to comparatively simple structures (i.e., few terms, interactions and restricted number of basis functions), reducing the potential for choosing over-fitted models without formal comparison. AIC is calculated as:

$$AIC = -2\log(L) \cdot 2k \quad (11)$$

where L is the maximum likelihood estimate, and k is the number of parameters. Where any two comparable models had a $|\Delta AIC| > 10$, we considered the model with the lower score more suitable. We chose to carry out the analysis in its current form rather than on considerably smaller but comparable sample sizes across models, to identify the strongest relationships in the existing data. This allowed us to highlight the utility of the approach per se and for Berlin in particular. Lastly, we also report the root mean squared error ($RMSE = \sqrt{\frac{1}{n} \sum_{i=1}^n (y_i - \hat{y}_i)^2}$) and mean absolute error ($MAE = \frac{1}{n} |y_i - \hat{y}_i|$) for the final model.

Results

Growth trend dynamics

Recently established annual, incremental growth is on average greater as compared to earlier times (i.e., prior 1960; Fig. 3). The contrast is strongest in the first 30 years of cambial development, with clear indication that averages are statistically different up to approximately 22 years (cf. overlap of 95% confidence intervals). The predicted trajectories for both periods follow typical ontogenetic patterns, yet differ in shape. This may be due to inaccurately estimated cambial ages, explaining the largely monotonic decrease for recent growth due to missing the typical (but not always present) initial rise and fall in pith-near stages. This would inadvertently create a left-shift in Fig. 3 for recent growth. Assuming that to be the case, the actual difference in average rates would be greater than presented here.

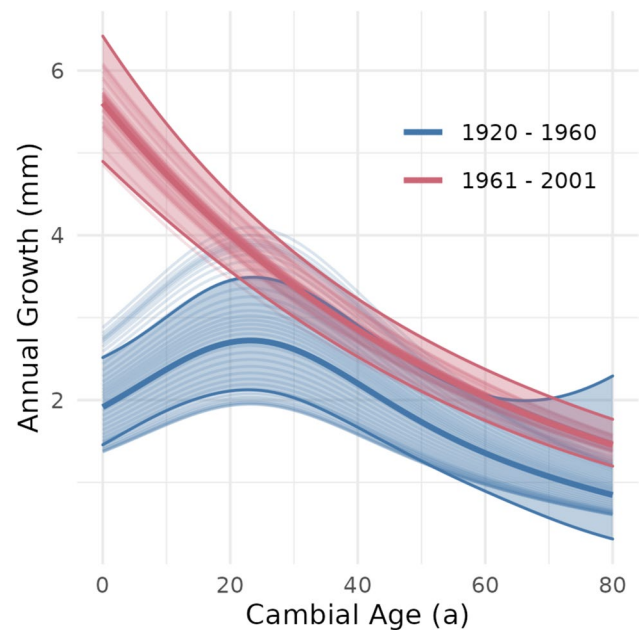


Fig. 3 Rates for annual incremental growth differ between recent and earlier times, as predicted by a hierarchical GAM (see Section [Dendrochronological analyses](#)). Thick lines and bands are for mean and 95% confidence interval of all annual predictions across a time group (fine lines). On average, early stages of recent growth (up to approximately 22 years) exceed that of earlier periods discernibly

Model selection

The null models containing only age to explain diameter captured a large portion of deviance. Including additional covariates thus resulted only in comparatively small increases of predictive skill. The inclusion of temperature (additive structure) and temperature-age interactions improved the predictive skill, with interactions reaching higher explained deviance (i.e., skill). Models including the MODIS-derived UHI measures performed best on average, where models containing $LCZ6_{150m}$ or all covariates (saturated model) did best (Fig. 4), which also holds true for other temperature/UHI measures. Note that non-temperature models containing planting bed area and $LCZ6_{150m}$ alone outperformed several of those including other temperature measures and covariate combinations. This indicated the importance of both covariates, with $LCZ6_{150m}$ also represented in the best-performing model, corroborating its impact on stem diameter development. As $LCZ6_{300m}$ only marginally increased performance compared to the null model (age only), the reference scale for the impact of the urban fabric (i.e., LCZ6) likely has a limit at $< 300 m$. Nutrient availability, similar to $LCZ6_{300m}$, also only improved model performance marginally. Building height, regardless of its reference scale (i.e., 150 vs. 300 m),

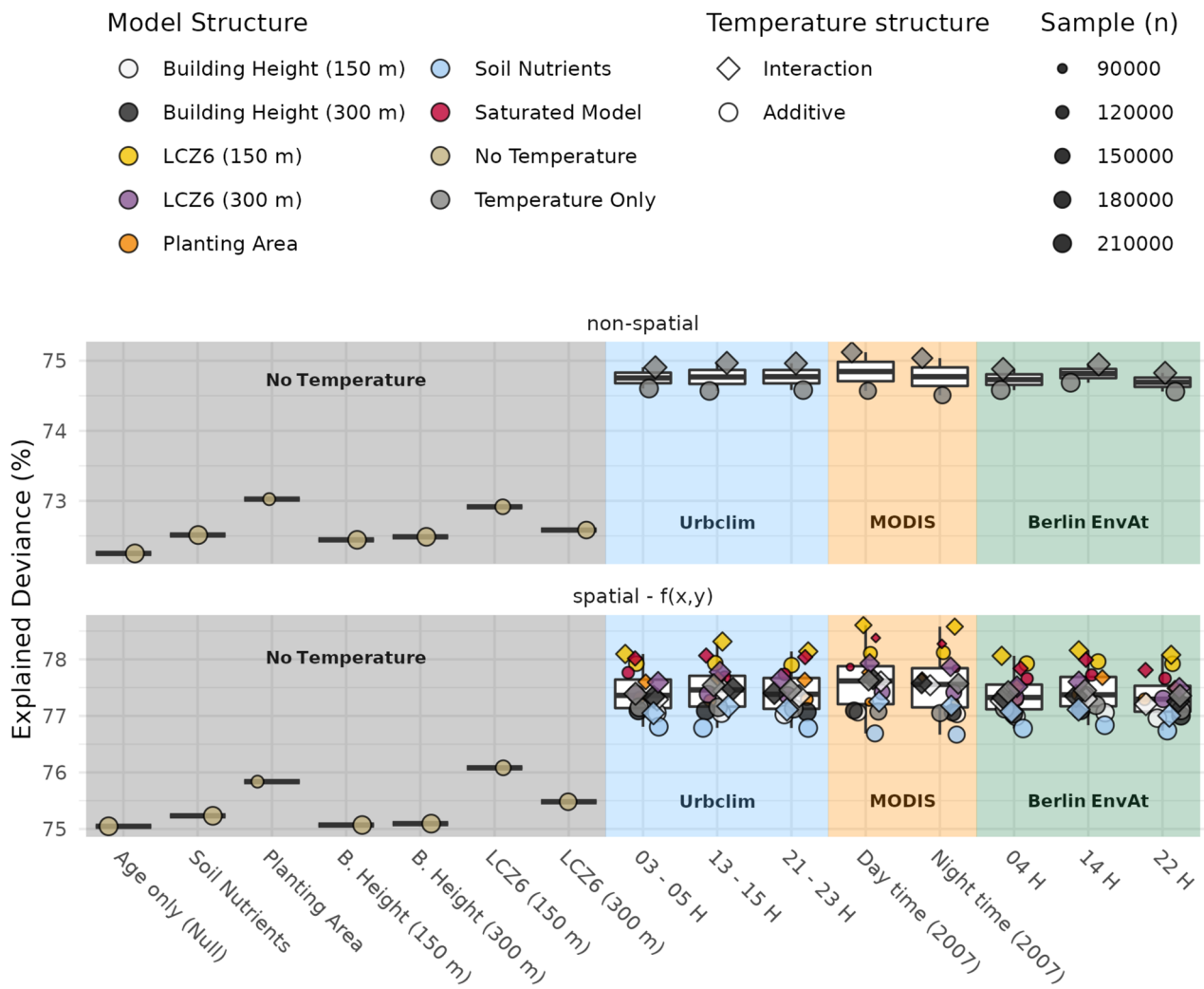


Fig. 4 Overview of model fit, expressed as explained deviance, for all tested models. The Panels distinguish between models without (top) and with (bottom) spatial smooths to account for autocorrelated residuals. Colored areas reflect (inclusion of) temperature and (excess) heat measures. Symbols identify models with an interaction between temperature and age (diamond), and without (circle), while symbol colors highlight covariates and their reference radius (i.e. 150/300m, but also note x-axis labels). Symbol size indicates the model's

included observations (i.e., sample size). Generally, including temperature (interactions) improves model fits above the null model (age only) and other non-temperature models. However, note the importance of planting bed area and LCZ6 cover is apparent even without including temperature. The MODIS-derived UHI measures provide the best fit on average, with the model including a temperature-age interaction and LCZ6 cover scoring highest overall

as another proxy for urban fabric, showed minimal to no improvement compared to the age-only null model.

Differences in sample sizes between model structures due to covariate and/or temperature data coverage were considerable (e.g., planting bed area vs. soil nutrient models for Urb-Clim UHI). Thus, we considered the model with the overall greatest predictive skill and largest sample for further investigations, namely $LCZ6_{150m}$ for MODIS derived UHI. For this variable combination, the model structure with age and temperature interaction also had a lower AIC ($AIC = 8.95 \cdot 10^5$) compared to the additive one ($AIC = 8.98 \cdot 10^5$).

The final model, comprising a temperature-age interaction, the covariate $LCZ6_{150m}$ and MODIS-derived UHI following Eq. (6), showed good agreement between predicted and observed *DBH* for the majority of observations (Fig. 5; $R^2 = 0.79$) resulting in a fairly low MAE of 6.12 cm, and a RMSE of $1.2 \cdot 10^{-9}$ cm. While some prediction errors are large (spread in Fig. 5), the predictions are unbiased (see correspondence of 1:1 and least-squares fit in Fig. 5). Thus, we consider using species and age-group averages as appropriate for identifying and discussing relationships between *DBH* and other covariates.

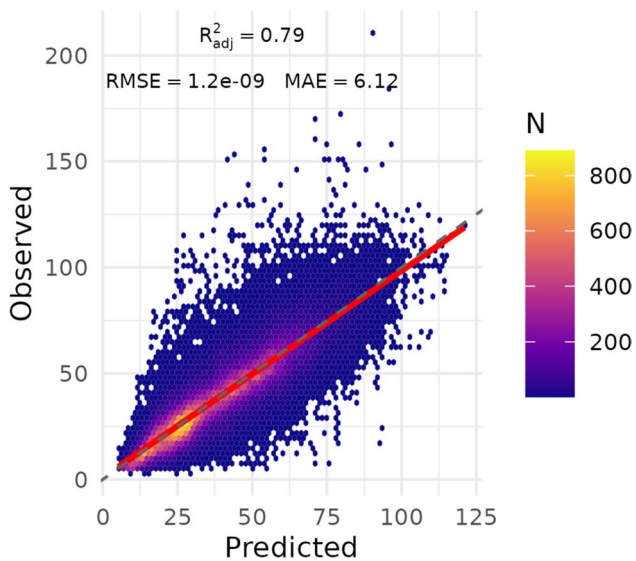


Fig. 5 Predicted vs. observed data for the best model according to explained deviance and AIC comparison, based on the MODIS-derived UHI measure (Chakraborty and Lee 2019) for average summer conditions (2007) and LCZ6 (open to mid-rise, Stewart and Oke 2012). Hexagons and colors represent x-y bins (i.e., in the observed-predicted space) and their counts (N), and the red line is a least-squares fit. The model captures the mean response well, as indicated by lighter colors along the dashed 1:1 line, and its close approximation by the least squares fit, as well as model metrics (see text label in figure)

Urban heat and urban fabric effects on stem growth

Relationships derived via the GAM in Eq. (6) with LCZ6 as covariate show fairly consistent responses across age groups considering trajectories, yet they differ somewhat in shape (Fig. 6) and considerably in absolute magnitude (i.e., slope in Fig. 7). Generally, younger age groups (30–35) showed increased growth (strongest for *A. hippocastanum*, *T. intermedia*, *T. intermedia* ‘Pallida’), or little to no impact (*Acer platanoides*, *Acer pseudoplatanus*), with stronger UHI magnitude. At older ages, this trajectory gradually shifted toward decreasing stem diameter at higher temperatures, with *T. euchlora*, *A. pseudoplatanus* and *P. acerifolia* having the most negative relationships. Notably, *Platanus acerifolia* showed an earlier reversal of sensitivity at age group 45–50 as compared to other species. This may be due to the stronger upward curvature towards the estimates’ lower temperature limit (see respective panel in Fig. 6). Although the uncertainty around this edge is comparatively well-constrained, the low number of observations at the end of the continuum does call for caution for further interpretation.

The distribution of individual street trees along the UHI continuum, evident in the density estimates in Fig. 6, show that the majority of species investigated here are subjected to intermediate to high UHI levels. Trees in younger age

groups are typically further toward the upper end of this continuum. Several species - including *A. platanoides*, *A. pseudoplatanus*, *Acer hippocastanum*, *Quercus robur*, and *Tilia euchlora* - have good coverage across the entire UHI continuum (although skewed toward positive values), which increases the confidence in the observed trajectory shift from young to old. Contrastingly, the cultivar *Tilia intermedia* ‘Pallida’ is predominantly distributed along the upper end of the continuum, resulting in greater uncertainty in the estimated relationship across age groups and UHI magnitudes.

The chosen model also highlighted that, on average, trees growing in less urbanized environments (i.e., more open to mid-rise urban land cover; LCZ6_{150 m}) achieve greater diameters (Fig. 8). Note, that planting bed area, similar to LCZ6_{150 m}, was identified as a covariate increasing explained deviance, both in models with and without a temperature measure, and represents an opportunity for further investigation, especially following additional data collection.

Discussion

Heat, environmental and urban controls on tree growth

Demographic patterns

We showed that initial growth rates ($\lesssim 30$ a) are greater in recently established trees, as compared to older ones. This pattern was found in annually-resolved incremental growth observations, and corresponds with prior work on urban-rural (e.g., Pretzsch et al. 2017; Zhao et al. 2016) and intra-urban comparisons (e.g., Dahlhausen et al. 2018), where it was attributed to increased temperatures - namely, the UHI effect. Furthermore, the space-for-time substitution highlighted that recently established, i.e. younger, trees have greater (positive) sensitivity to heat than intermediate age groups, while the oldest trees showed lower average absolute growth (diameters) with increasing heat. We are not aware of other studies reporting such an age-dependent shift in sensitivity. However, the consistency of this pattern across species provides a satisfactory level of confidence in it, and indeed, Dahlhausen et al. (2018) also report a time - and by implication an age-dependent - shift of temperature sensitivity on growth depending on urban development intensity, but do not further distinguish between age groups. The age-dependent shift may be explained by a combination of physiological and environmental changes over time, and/or may be related to management practices, but we acknowledge that additional analyses is required to disentangle these processes. For instance, higher temperatures may have benefited physiological processes close to their respective optima in

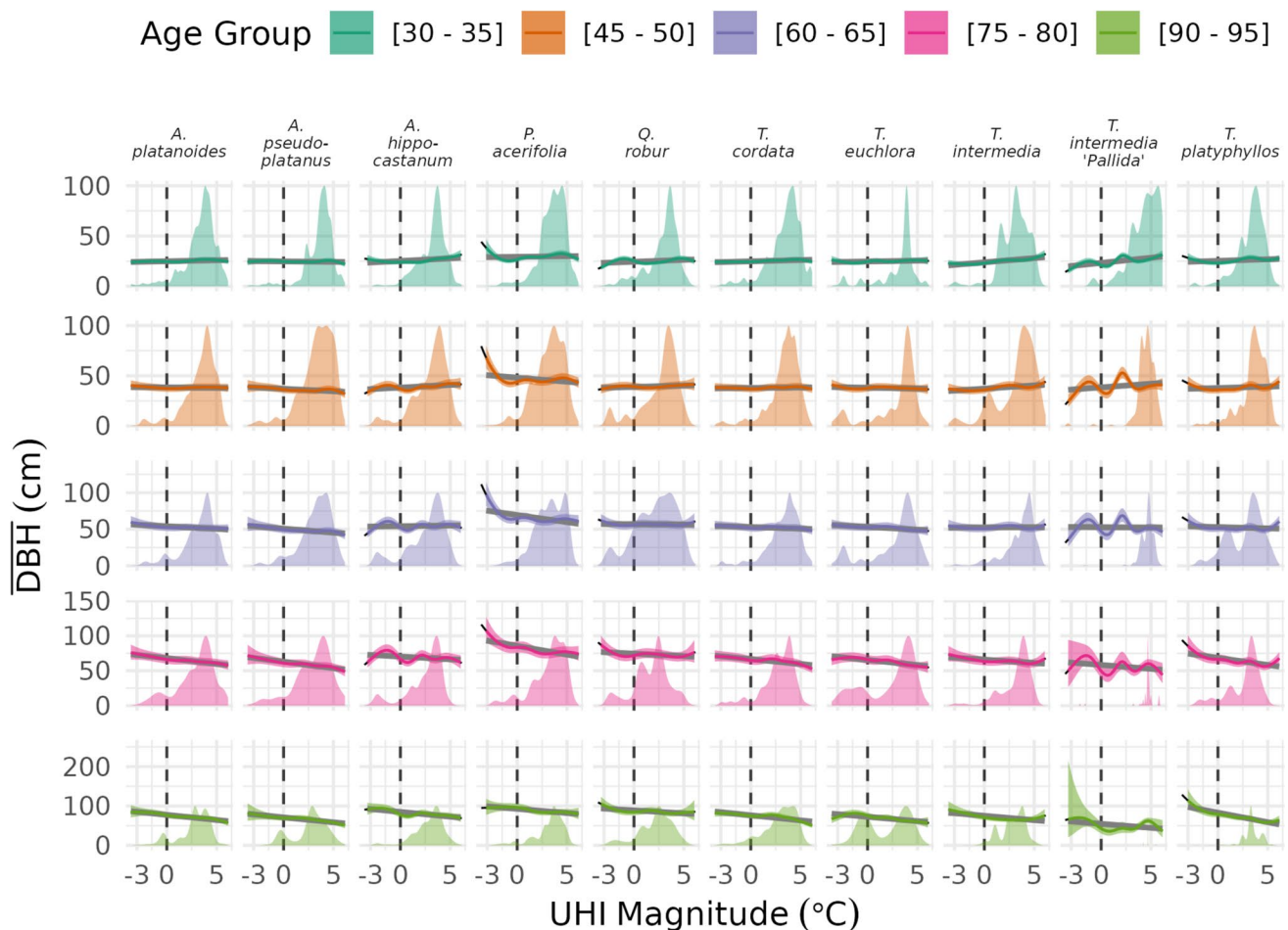


Fig. 6 Age-group averaged relationships between the MODIS-derived UHI and stem diameter for the ten most abundant species from the best model (i.e., Eq. (6) with LCZ6 as covariate). Note that estimates were derived with $LCZ6_{150\text{ m}} = 0.5$, and that y-axis scales differ between panel rows. The colored lines and bands are the averaged GAM fit, and gray lines are least-squares estimates fitted to

these averages. Estimates were only generated within temperature ranges that a given species experienced. Density plots (scaled to match 100cm on the y-axis) show the distribution of individual trees along the urban heat continuum, aiding both with interpreting uncertainties (band width, “wiggleness”) and assessing species’ exposure to urban heat. A general shift from increased or stable growth with temperature at younger ages to a decrease for older trees is apparent

both young and old individuals. But, as older trees must support greater leaf area through rooting in similarly small (restricted) soil volumes, water availability and nutrients may become increasingly limiting. Higher rates of transpiration and photosynthesis, driven through temperature increases, could thus turn detrimental as the ratios between soil volume, root and leaf area change throughout a trees life span and in time. In addition to this, younger trees are typically more rigorously managed and irrigated (e.g., Koeser et al. 2014), which may (further) alter age-dependent temperature sensitivity. We lack data on demographic differences in management to confirm this, and acknowledge that younger trees here also surpassed their establishment phase, which entails high mortality during the first five years after planting (Harris and Day 2017; Hilbert et al. 2019) during which the above would not apply.

Intra-specific differences

Generally, the ten investigated species and cultivars showed consistent responses in sign, but differed substantially in magnitude, modulated by age. *Aesculum hippocastanum*, *Tilia intermedia*, *T. intermedia* ‘pallida’ and showed greatest absolute growth at high temperatures at younger (30–35) as well as older ages (60–65). The drought tolerance and performance under high temperatures is well documented for the latter two and features in tree selection frameworks, such as species climate matrices in Roloff et al. (2009) and in Brune (2016), where several studies investigating (hydro) climatic sensitivity were summarized. Contrastingly, *Acer pseudoplatanus* showed decreased absolute growth with higher temperatures; this corresponds with their classification as *not very suitable* according to Roloff et al. (2009).

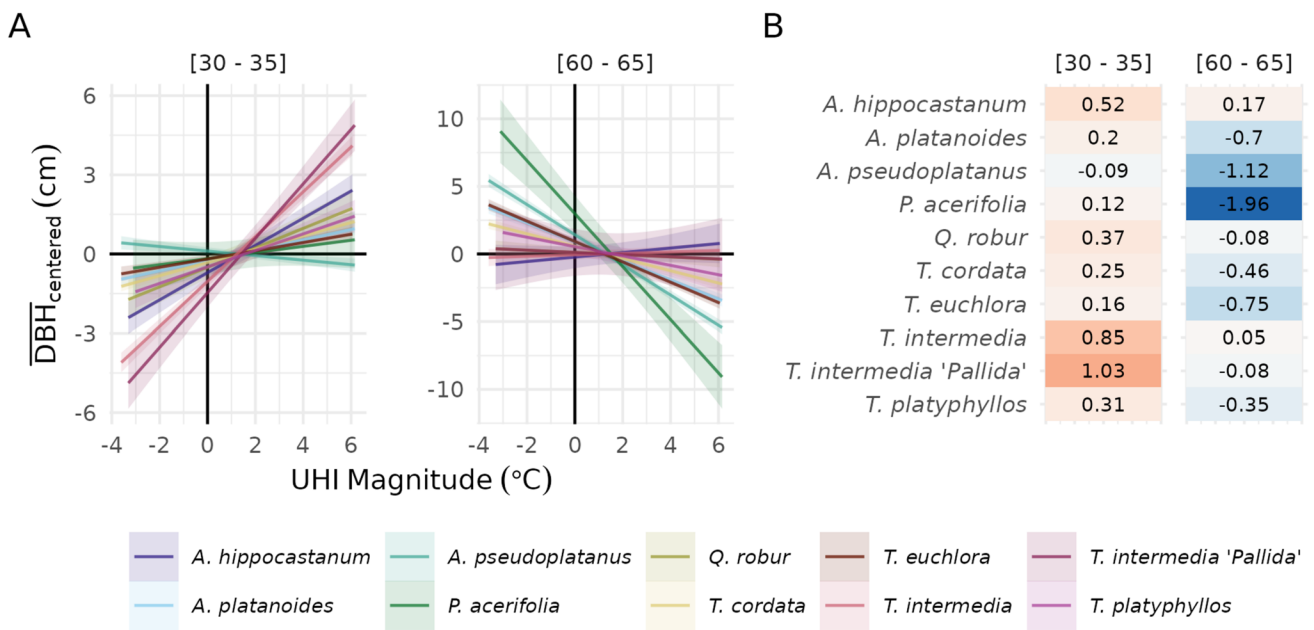


Fig. 7 Temperature sensitivity of diameter growth centered on species-specific means for comparability and to aid interpretation of inter-specific differences. Lines and bands are from ordinary least

squares fits on the GAM estimates in Fig. 6 (A) and the corresponding coefficients (slopes, B)

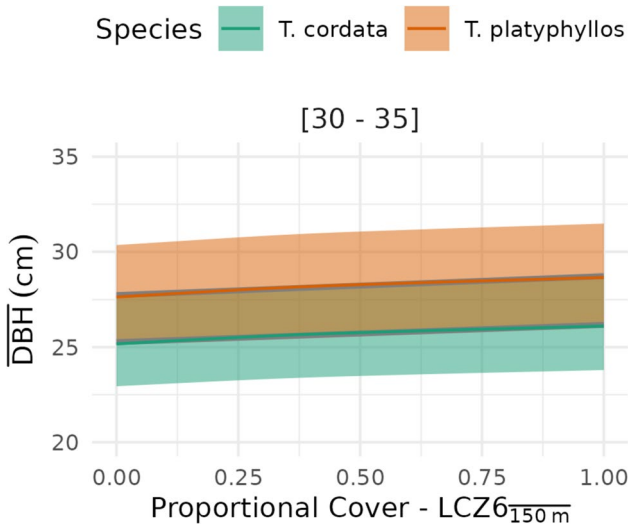


Fig. 8 Age-group averaged relationships between the LCZ6 and stem diameter for two *Tilia* genera from the best model (i.e., Eq. (6) with MODIS-derived UHI as excess heat measure). LCZ6 cover was derived as a weighted average within a radius of 150m around each tree. Note the identical shape, but difference in intercept as a result of the model specification with a global smooth for the non-temperature covariate for all species (see Section [Stem diameter model development and selection](#)); the UHI magnitude was fixed at 3 °C where most trees are present across age groups. The model identified a steady increase of average stem diameter with open to mid-rise urban land cover

Platanus acerifolia and *Acer platanoides* are considered *suitable* and *very suitable* (Roloff et al. 2009), yet show the greatest decline with temperatures here. Indeed, several studies reviewed in Brune (2016) highlight *A. platanoides* as drought-tolerant. Such contrasting indications are also given for *A. pseudoplatanus*, and even report *A. hippocastanum* as only moderately tolerant, despite performing best here. These differences may be due to idiosyncrasies of planting sites, such as low soil volume and increased potential for water stress, (long-term) interactions with pathogens and herbivores (e.g., Meineke and Frank 2018), or perhaps related to data quality. Most important, these differences highlight the need for assessments of performance (e.g., as growth) under location-specific conditions, and this study provides a first attempt and insights into temperature sensitivity at the scale of an entire metropolis.

Utility, transferability and limitations of approach

The major strength of this work is the estimation of growth sensitivity of urban trees to heat and other urban conditions at city-scale with little data and processing power requirements. In particular, differences within and between species across several dimensions (depending on model specification) are readily explored where only tree locations, age, diameter (or any other target) and selected variables

are needed to implement this approach. Indeed, due to the high temporal and spatial variability of controls on growth, and thus variability in responses, such assessments should be developed specifically for a given setting, as well-understood tree characteristics (e.g., Roloff et al. 2009), could be strongly mediated at a given location or time. For instance, if drought hardiness is related to extensive root networks, the limited soil volumes available to street trees could render a species vulnerable to water stress. In addition, studies on climatic suitability and physiological responses are difficult to compare due to local acclimation of species to controls on growth and performance, as well as different methodological protocols (e.g., see Brune 2016). Thus, the approach followed here, with its comparatively simple data requirements, can be implemented in a variety of settings to gain initial and/or guiding insights on tree performance in a specific urban region, and also serve as a benchmark to compare other empirical estimates or mechanistic models with. It may even allow estimating tree performance under future conditions to some extent (e.g., considering increase in temperature alone for this study), but is of course contingent on data coverage (e.g., demographics, environmental gradients). Furthermore, the implementation of GAM models here with `mgcv::bam()` is computationally efficient (Wood et al. 2017), making model testing, selection and final application a rapid process even for abundant observations (here $n > 150000$ and processing times of $t < 60$ s on a desktop computer for the selected model). Future research may focus on collecting additional data (e.g., increasing the coverage on planting bed area) and subsequently deriving species-specific smooths for ancillary environmental covariates.

Two noteworthy caveats of the approach followed here lie in its empirical, data-driven nature, and its dependence on data quality. The presented results here are correlative. While their interpretation follows first principles and may also allow anticipating the performance of a given tree under a range of increased temperatures, insights derived from mechanistic understanding are indispensable. This is because a change in one environmental condition, e.g., temperature or pest abundance, may also entail alterations to other drivers, and ultimately, affect physiological processes in ways not yet captured in existing data. Furthermore, the data provided in Berlin's tree inventory required extensive quality controlling, and it is likely that inaccurate (diameter, age) or interpolated (diameter) observations were including in the analyses. However, the minimum requirement of 10000 observations per species, and the focus on average diameter responses across age groups decreased potential impacts of such observations to a degree that was considered satisfactory, while uncertainty is communicated effectively and transparently (i.e., larger confidence bands for *T. intermedia* 'Pallida'). Further, the utility and transferability of the approach per se were considered of value to the community and practitioners.

Implications

Tree species selection for urban forests and urban greening depends on several often competing factors - such as aesthetic appeal and ecosystem service provision (e.g., Roman et al. 2020) - and has been focused on identifying trees suitable for current and future conditions for the last decades with increasingly strong evidence basis (e.g., Hirons and Sjöman 2019). Here, biogeographical approaches aim to match natural (i.e., non-urban) species distributions within current bioclimatic envelopes with future conditions at a planting site (e.g., Broadmeadow et al. 2005). Watkins et al. (2020) used such "climate matching" to identify the space along environmental dimensions (heat, precipitation) which urban regions inhabit, falling within or extending the natural envelope. Our work extends this approach by identifying the heat space (i.e., UHI range) occupied by several key species within a city. This not only allows identifying species-specific and intra-specific (age-dependent) sensitivities to urban conditions, but can also inform how age cohorts may respond as temperatures at a given location shift along the present continuum through time, while accounting for the impacts of additional urban conditions (e.g., management, disturbance, urban fabric). Notably, increased growth rates at higher temperatures, as reported here, also entail greater demographic turnover through mortality (Smith et al. 2019). Thus, as the majority of individuals were situated at the upper end of the temperature continuum, high temperature sensitivity may entail additional management due to faster turn-over and potentially subsequent replacement by more appropriate species. In addition, our approach can allow managers and planners to identify potential scale-limits of the urban fabric (e.g., $LCZ6_{150\ m}$ vs. $LCZ6_{300\ m}$) on tree performance when altering surroundings or planting in a given area; efforts should be directed toward identifying the most pertinent environmental covariates and how their influence scales in space. The insights derived from this study, and potentially others following this approach in the future, can therefore add another dimension to tree selection approaches implemented down to individual trees and locations. It thus complements quantitative and qualitative tools, such as the climate matching tool, ecological site classification or species-climate matrix (see Hirons and Sjöman (2019); Roloff et al. (2009); Brune (2016); and references therein).

Finally, open data was key for this study. We urge authorities to implement FAIR (findable, accessible, inter-operable and reusable) data principles to enable work similar to ours, as well as the creation of larger-scale, multi-temporal databases and/or execution of synoptic studies (e.g., Ossola et al. 2020). This also includes the collection and provision of standardized (meta) data for quality control and to improve statistical inference.

Conclusion

We showcased the application of a GAM-driven analyses to identify the sensitivity of urban tree growth to environmental and urban drivers in a space-for-time framework. The extensive data coverage (tree inventory and covariates) allowed us to account for location-specific influences and identify the factors with strongest impacts on growth potentials (i.e., maximum diameter) for individual species. The identified age-dependent shift of temperature sensitivity, which was fairly consistent across species, as well as inter-specific differences thereof, will inform and guide further research. Notably, increasing the confidence in and coverage of data collection on less abundant species is key to maximize the potential of the approach developed here. Our results are a contribution toward Berlin's current and future management of its tree stock and may help drive adaptation to climate change. Despite being a case study for a single city, we believe our work may provide a flexible approach for other cities with available or growing inventories, as well as ancillary environmental data, and may also inform the use of other planning tools, such as species-climate matrices (Roloff et al. 2009) regarding temperature sensitivity.

Supplementary Information The online version contains supplementary material available at <https://doi.org/10.1007/s11252-023-01450-9>.

Acknowledgements AGH and IH were supported through the Helmholtz-Climate-Initiative (HI-CAM), funded by the Helmholtz Initiative and Networking Fund. We thank Prof Dr Christoph Schneider and Dr Burkhard Neuwirth for providing dendrochronological data, as well as Berlin's senate for providing FAIR data and support for its use. The comments of two anonymous referees are greatly appreciated.

Author contributions A.G.H.: Conceptualization, Methodology, Data curation, Formal analysis, Visualization, Writing - Original Draft. I. H.: Resources, Investigation, Project administration, Funding acquisition, Writing - Review & Editing.

Funding Open Access funding enabled and organized by Projekt DEAL. AGH and IH were supported through the Helmholtz-Climate-Initiative (HI-CAM), funded by the Helmholtz Initiative and Networking Fund; the authors are responsible for the content of this publication.

Data Availability and Code All code to reproduce the analyses and manuscript are archived on Zenodo as: Alexander Hurley et al. (2022). the-Hull/berlin.trees: UE Submission (v1.0.0). Zenodo. <https://doi.org/10.5281/zenodo.7217032>. This code includes routines to download and process data from public repositories, with sources listed in the Section **Data sources** in **Methods**. The list of sources includes additional data sets, which were manually downloaded, but were too large to archive online. Data for the dendrochronological analyses is available in the Zenodo archive.

Declarations

Ethics approval Not applicable.

Competing interests The authors declare no competing interests.

Open Access This article is licensed under a Creative Commons Attribution 4.0 International License, which permits use, sharing, adaptation, distribution and reproduction in any medium or format, as long as you give appropriate credit to the original author(s) and the source, provide a link to the Creative Commons licence, and indicate if changes were made. The images or other third party material in this article are included in the article's Creative Commons licence, unless indicated otherwise in a credit line to the material. If material is not included in the article's Creative Commons licence and your intended use is not permitted by statutory regulation or exceeds the permitted use, you will need to obtain permission directly from the copyright holder. To view a copy of this licence, visit <http://creativecommons.org/licenses/by/4.0/>.

References

- Arcus VL, Prentice EJ, Hobbs JK, Mulholland AJ, Van der Kamp MW, Pudney CR, Parker EJ, Schipper LA (2016) On the temperature dependence of enzyme-catalyzed Rates. *Biochemistry* 55:1681–1688. <https://doi.org/10.1021/acs.biochem.5b01094>
- Au KN (2018) An integrated approach to tree stress monitoring. *Arborist News*, International Society of Arboriculture 27:28–31
- Beck HE, Zimmermann NE, McVicar TR, Vergopolan N, Berg A, Wood EF (2018) Present and future Köppen-Geiger climate classification maps at 1-km resolution. *Sci Data* 5:180214. <https://doi.org/10.1038/sdata.2018.214>
- Begum S, Nakaba S, Yamagishi Y, Oribe Y, Funada R (2013) Regulation of cambial activity in relation to environmental conditions: understanding the role of temperature in wood formation of trees. *Physiol Plant* 147:46–54. <https://doi.org/10.1111/j.1399-3054.2012.01663.x>
- Berland A (2020) Urban tree growth models for two nearby cities show notable differences. *Urban Ecosyst* 23:1253–1261. <https://doi.org/10.1007/s11252-020-01015-0>
- Briber BM, Hutyra LR, Reinmann AB, Raciti SM, Dearborn VK, Holden CE, Dunn AL (2015) Tree productivity enhanced with conversion from forest to urban land covers. *PLoS ONE* 10. <https://doi.org/10.1371/journal.pone.0136237>
- Broadmeadow MSJ, Ray D, Samuel CJA (2005) Climate change and the future for broadleaved tree species in Britain. *Forest Int J For Res* 78:145–161. <https://doi.org/10.1093/forestry/cpi014>
- Brune M (2016) Urban trees under climate change. Potential impacts of dry spells and heat waves in three german regions in the 2050s (no. Report 24). Climate Service Center Germany, Hamburg
- Chakraborty T, Lee X (2019) A simplified urban-extent algorithm to characterize surface urban heat islands on a global scale and examine vegetation control on their spatiotemporal variability. *Int J Appl Earth Obs Geoinf* 74:269–280. <https://doi.org/10.1016/j.jag.2018.09.015>
- Core Team R (2021) R: a language and environment for statistical computing. R Foundation for Statistical Computing, Vienna, Austria
- Dahlhausen J, Rötzer T, Biber P, Uhl E, Pretzsch H (2018) Urban climate modifies tree growth in Berlin. *Int J Biometeorol* 62:795–808. <https://doi.org/10.1007/s00484-017-1481-3>
- Dale AG, Frank SD (2014) The effects of urban warming on herbivore abundance and street tree condition. *PLOS ONE* 9:e102996. <https://doi.org/10.1371/journal.pone.0102996>
- De Ridder K, Lauwaet D, Maiheu B (2015) UrbClim – A fast urban boundary layer climate model. *Urban Clim* 12:21–48. <https://doi.org/10.1016/j.uclim.2015.01.001>
- Demuzere M, Bechtel B, Middel A, Mills G (2019) Mapping Europe into local climate zones. *PLoS ONE* 14. <https://doi.org/10.1371/journal.pone.0214474>

- Dusenge ME, Duarte AG, Way DA (2019) Plant carbon metabolism and climate change: elevated CO₂ and temperature impacts on photosynthesis, photorespiration and respiration. *New Phytol* 221:32–49. <https://doi.org/10.1111/nph.15283>
- Fatichi S, Leuzinger S, Körner C (2014) Moving beyond photosynthesis: from carbon source to sink-driven vegetation modeling. *New Phytol* 201:1086–1095. <https://doi.org/10.1111/nph.12614>
- Fenner D, Meier F, Scherer D, Polze A (2014) Spatial and temporal air temperature variability in Berlin, Germany, during the years 2001–2010. *Urban Clim ICUC8: 8th Int Conf Urban Clim 10th Symp Urban Environ* 10 308:331. <https://doi.org/10.1016/j.uclim.2014.02.004>
- Fritts HC, Swetnam TW (1989) Dendroecology: a tool for evaluating variations in past and present forest environments. *Adv Ecol Res* 19:111–188
- Geange SR, Arnold PA, Catling AA, Coast O, Cook AM, Gowland KM, Leigh A, Notarnicola RF, Posch BC, Venn SE, Zhu L, Nicotra AB (2021) The thermal tolerance of photosynthetic tissues: a global systematic review and agenda for future research. *New Phytol* 229:2497–2513. <https://doi.org/10.1111/nph.17052>
- Gillner S, Bräuning A, Roloff A (2014) Dendrochronological analysis of urban trees: climatic response and impact of drought on frequently used tree species. *Trees* 28:1079–1093. <https://doi.org/10.1007/s00468-014-1019-9>
- Gross G (1994) Project WIND Numerical Simulations with FIT-NAH. In: Pielke RA, Pearce RP (eds) *Mesoscale modeling of the Atmosphere, Meteorological Monographs*. American Meteorological Society, Boston, MA, pp 73–80. https://doi.org/10.1007/978-1-935704-12-6_9
- Grossiord C, Buckley TN, Cernusak LA, Novick KA, Poulter B, Siegwolf RTW, Sperry JS, McDowell NG (2020) Plant responses to rising vapor pressure deficit. *New Phytol* 226:1550–1566. <https://doi.org/10.1111/nph.16485>
- Hansen R, Olafsson AS, van der Jagt APN, Rall E, Pauleit S (2019) Planning multifunctional green infrastructure for compact cities: what is the state of practice? *Ecological indicators, from urban sprawl to compact green cities – indicators for multi-scale and multi-dimensional Anal* 96:99–110. <https://doi.org/10.1016/j.ecolind.2017.09.042>
- Harris JR, Day SD (2017) Navigating the establishment period: a critical period for new trees. In: *Routledge Handbook of Urban Forestry*. Routledge
- Hastie TJ, Tibshirani RJ (2017) *Generalized additive models*. Routledge
- Hertel D, Schlink U (2019) Decomposition of urban temperatures for targeted climate change adaptation. *Environ Model Softw* 113:20–28. <https://doi.org/10.1016/j.envsoft.2018.11.015>
- Hilbert DR, Roman LA, Koeser AK, Vogt J, van Doorn NS (2019) Urban tree mortality: What the literature shows us. *Arborist News*. Oct: 22–26. Oct, 22–26
- Hirons A, Sjöman H (2019) Tree species selection for green infrastructure: a guide for specifiers. *Trees and Design Action Group*
- Holmes RL, Adams RK, Fritts HC (1986) Tree-ring chronologies of western North America: California, eastern Oregon and northern Great Basin with procedures used in the chronology development work including users manuals for computer programs COFECHA and ARSTAN
- Hurley AG, Peters RL, Pappas C, Steger DN, Heinrich I (2022) Addressing the need for interactive, efficient, and reproducible data processing in ecology with the dataclean R package. *PLoS ONE* 17. <https://doi.org/10.1371/journal.pone.0268426>
- Jia W, Zhao S, Liu S (2018) Vegetation growth enhancement in urban environments of the Conterminous United States. *Glob Change Biol* 24:4084–4094. <https://doi.org/10.1111/gcb.14317>
- Koeser AK, Gilman EF, Paz M, Harchick C (2014) Factors influencing urban tree planting program growth and survival in Florida, United States. *Urban For Urban Green* 13:655–661. <https://doi.org/10.1016/j.ufug.2014.06.005>
- Körner C (2015) Paradigm shift in plant growth control. *Curr Opin Plant Biol* 25:107–114. <https://doi.org/10.1016/j.pbi.2015.05.003>
- Kuttler W, Miethke A, Düttemeyer D, Barlag A-B (eds) (2015) *Das klima von essen = the climate of essen*. Westarp Wiss, Hohenwarsleben
- Lauwaet D, De Ridder K, Saeed S, Brisson E, Chatterjee F, van Lipzig NPM, Maiheu B, Hooyberghs H (2016) Assessing the current and future urban heat island of Brussels. *Urban Clim* 15:1–15. <https://doi.org/10.1016/j.uclim.2015.11.008>
- Li Z, Wood SN (2020) Faster model matrix crossproducts for large generalized linear models with discretized covariates. *Stat Comput* 30:19–25. <https://doi.org/10.1007/s11222-019-09864-2>
- Locosselli GM, Camargo EPD, Moreira TCL, Todesco E, Andrade MDF, André CDS, André PAD, Singer JM, Ferreira LS, Saldiva PHN, Buckeridge MS (2019) The role of air pollution and climate on the growth of urban trees. *Sci Total Environ* 666:652–661. <https://doi.org/10.1016/j.scitotenv.2019.02.291>
- Long SP (1991) Modification of the response of photosynthetic productivity to rising temperature by atmospheric CO₂ concentrations: has its importance been underestimated? *Plant Cell Environ* 14:729–739. <https://doi.org/10.1111/j.1365-3040.1991.tb01439.x>
- McDowell N, Pockman WT, Allen CD, Breshears DD, Cobb N, Kolb T, Plaut J, Sperry J, West A, Williams DG, Yezpe EA (2008) Mechanisms of plant survival and mortality during drought: why do some plants survive while others succumb to drought? *New Phytol* 178:719–739. <https://doi.org/10.1111/j.1469-8137.2008.02436.x>
- Meineke EK, Frank SD (2018) Water availability drives urban tree growth responses to herbivory and warming. *J Appl Ecol* 55:1701–1713. <https://doi.org/10.1111/1365-2664.13130>
- Mohamed MA (2017) Monitoring of temporal and spatial changes of land use and land cover in metropolitan regions through remote sensing and GIS. *NR* 08:353–369. <https://doi.org/10.4236/nr.2017.85022>
- Monteiro R, Ferreira JC, Antunes P (2020) Green infrastructure planning principles: An integrated literature review *land* 9:525. <https://doi.org/10.3390/land9120525>
- Moser-Reischl A, Rahman MA, Pauleit S, Pretzsch H, Rötzer T (2019) Growth patterns and effects of urban micro-climate on two physiologically contrasting urban tree species. *Landsc Urban Plann* 183:88–99. <https://doi.org/10.1016/j.landurbplan.2018.11.004>
- Norton BA, Coutts AM, Livesley SJ, Harris RJ, Hunter AM, Williams NSG (2015) Planning for cooler cities: a framework to prioritise green infrastructure to mitigate high temperatures in urban landscapes. *Landsc Urban Plann* 134:127–138. <https://doi.org/10.1016/j.landurbplan.2014.10.018>
- O'Brien AM, Ettinger AK, HilleRisLambers J (2012) Conifer growth and reproduction in urban forest fragments: predictors of future responses to global change? *Urban Ecosyst* 15:879–891. <https://doi.org/10.1007/s11252-012-0250-7>
- Oke TR (1982) The energetic basis of the urban heat island. *Q J R Meteorol Soc* 108:1–24. <https://doi.org/10.1002/qj.49710845502>
- Oke TR (1992) *Boundary layer climates*. Routledge, London; New York
- Ossola A, Hoepfner MJ, Burley HM, Gallagher RV, Beaumont LJ, Leishman MR (2020) The Global Urban Tree Inventory: a database of the diverse tree flora that inhabits the world's cities. *Glob Ecol Biogeogr* 29:1907–1914. <https://doi.org/10.1111/geb.13169>
- Parent B, Turc O, Gibon Y, Stitt M, Tardieu F (2010) Modelling temperature-compensated physiological rates, based on the co-ordination of responses to temperature of developmental processes. *J Exp Bot* 61:2057–2069. <https://doi.org/10.1093/jxb/erq003>

- Pauleit S, Jones N, Garcia-Martin G, Garcia-Valdecantos JL, Rivière LM, Vidal-Beaudet L, Bodson M, Randrup TB (2002) Tree establishment practice in towns and cities – results from a European survey. *Urban For Urban Green* 1:83–96. <https://doi.org/10.1078/1618-8667-00009>
- Pedersen EJ, Miller DL, Simpson GL, Ross N (2019) Hierarchical generalized additive models in ecology: an introduction with mgcv. *PeerJ* 7. <https://doi.org/10.7717/peerj.6876>
- Peters RL, Steppe K, Cuny HE, De Pauw DJW, Frank DC, Schaub M, Rathgeber CBK, Cabon A, Fonti P (2021) Turgor – a limiting factor for radial growth in mature conifers along an elevational gradient. *New Phytol* 229:213–229. <https://doi.org/10.1111/nph.16872>
- Pinheiro J, Bates D, DebRoy S, Sarkar D, Core Team R (2021) *Nlme: Linear and nonlinear mixed effects models*
- Pretzsch H, Biber P, Uhl E, Dahlhausen J, Schütze G, Perkins D, Rötzer T, Caldentey J, Koike T, van Con T, Chavanne A, Toit B, du, Foster K, Lefer B (2017) Climate change accelerates growth of urban trees in metropolises worldwide. *Sci Rep* 7:1–10. <https://doi.org/10.1038/s41598-017-14831-w>
- Quigley MF (2004) Street trees and rural conspecifics: will long-lived trees reach full size in urban conditions? *Urban Ecosyst* 7:29–39. <https://doi.org/10.1023/B:UECO.0000020170.58404.e9>
- Randrup TB, McPherson EG, Costello LR (2001) A review of tree root conflicts with sidewalks, curbs, and roads. *Urban Ecosyst* 5:209–225. <https://doi.org/10.1023/A:1024046004731>
- Rathgeber CBK, Cuny HE, Fonti P (2016) Biological basis of Tree-Ring formation: a Crash Course. *Front. Plant Sci* 7. <https://doi.org/10.3389/fpls.2016.00734>
- Rhoades RW, Stipes RJ (1999) Growth of trees on the Virginia Tech campus in response to various factors 7
- Roloff A, Korn S, Gillner S (2009) The climate-species-matrix to select tree species for urban habitats considering climate change. *Urban For Urban Green* 8:295–308. <https://doi.org/10.1016/j.ufug.2009.08.002>
- Roman LA, Conway TM, Eisenman TS, Koeser AK, Barona CO, Locke DH, Jenerette GD, Östberg J, Vogt J (2020) Beyond 'trees are good': disservices, management costs, and tradeoffs in urban forestry. *Ambio* 21:183. <https://doi.org/10.1007/s13280-020-01396-8>
- Sarkar A, De Ridder K (2011) The urban heat island intensity of Paris: a case study based on a simple urban surface parametrization. *Boundary-Layer Meteorol* 138:511–520. <https://doi.org/10.1007/s10546-010-9568-y>
- Schneider C, Neuwirth B, Schneider S, Balanzategui D, Elsholz S, Fenner D, Meier F, Heinrich I (2021) Using the dendro-climatological signal of urban trees as a measure of urbanization and urban heat island. *Urban Ecosyst*. <https://doi.org/10.1007/s11252-021-01196-2>
- Smith IA, Dearborn VK, Hutyrá LR (2019) Live fast, die young: accelerated growth, mortality, and turnover in street trees. *PLoS ONE* 14. <https://doi.org/10.1371/journal.pone.0215846>
- Stewart ID (2011) A systematic review and scientific critique of methodology in modern urban heat island literature. *Int J Climatol* 31:200–217. <https://doi.org/10.1002/joc.2141>
- Stewart ID, Oke TR (2012) Local climate zones for urban temperature studies. *Bull Am Meteorol Soc* 93:1879–1900. <https://doi.org/10.1175/BAMS-D-11-00019.1>
- SUVK, Berlin (2019) Anteil öffentlicher Grünflächen in Berlin, Grünflächeninformationssystem (GRIS). Senatsverwaltung für Umwelt, Verkehr und Klimaschutz Berlin. Referat Freiraumplanung und Stadtgrün, Berlin
- Tjoelker MG, Oleksyn J, Reich PB (2001) Modelling respiration of vegetation: evidence for a general temperature-dependent Q10. *Glob Change Biol* 7:223–230. <https://doi.org/10.1046/j.1365-2486.2001.00397.x>
- Vo TT, Hu L (2021) Diurnal evolution of urban tree temperature at a city scale. *Sci Rep* 11:10491. <https://doi.org/10.1038/s41598-021-89972-0>
- Ward KT, Johnson GR (2007) Geospatial methods provide timely and comprehensive urban forest information. *Urban For Urban Green* 6:15–22
- Watkins JHR, Cameron RWF, Sjöman H, Hitchmough JD (2020) Using big data to improve ecotype matching for magnolias in urban forestry. *Urban For Urban Green* 48:126580. <https://doi.org/10.1016/j.ufug.2019.126580>
- Wohlfahrt G, Tomelleri E, Hammerle A (2019) The urban imprint on plant phenology. *Nat Ecol Evol* 3:1668–1674. <https://doi.org/10.1038/s41559-019-1017-9>
- Wood SN (2017) *Generalized additive models: an introduction with R*. CRC Press
- Wood SN (2006) Low-rank scale-invariant Tensor product smooths for generalized additive mixed models. *Biometrics* 62:1025–1036. <https://doi.org/10.1111/j.1541-0420.2006.00574.x>
- Wood SN, Li Z, Shaddick G, Augustin NH (2017) Generalized additive models for Gigadata: modeling the U.K. black smoke Network Daily Data. *J Am Stat Assoc* 112:1199–1210. <https://doi.org/10.1080/01621459.2016.1195744>
- Yamori W, Hikosaka K, Way DA (2014) Temperature response of photosynthesis in C3, C4, and CAM plants: temperature acclimation and temperature adaptation. *Photosynth Res* 119:101–117. <https://doi.org/10.1007/s11120-013-9874-6>
- Zhao S, Liu S, Zhou D (2016) Prevalent vegetation growth enhancement in urban environment. *PNAS* 113:6313–6318. <https://doi.org/10.1073/pnas.1602312113>
- Zhou B, Lauwaet D, Hooyberghs H, Ridder KD, Kropp JP, Rybski D (2016) Assessing seasonality in the surface urban heat island of London. *J Appl Meteorol Climatol* 55:493–505. <https://doi.org/10.1175/JAMC-D-15-0041.1>

Publisher's Note Springer Nature remains neutral with regard to jurisdictional claims in published maps and institutional affiliations.